JACS
JOURNAL OF THE AMERICAN CHEMICAL SOCIETY
Article
pubs.acs.org/JACS

Molecular Insights into Clathrate Hydrate Nucleation at an Ice–Solution Interface

Payman Pirzadeh and Peter G. Kusalik*

Department of Chemistry, University of Calgary, Calgary, Alberta, Canada

Supporting Information

ABSTRACT: Clathrate hydrates are specific cage-like structures formed by water molecules around a guest molecule. Despite the many studies that have been performed on clathrate hydrates, the actual molecular mechanism of both their homogeneous and heterogeneous nucleation has yet to be fully clarified. Here, by means of molecular simulations, we demonstrate how the interface of hexagonal ice can facilitate the heterogeneous nucleation of methane clathrate hydrate from an aqueous methane solution. Our results indicate an initial accumulation of methane molecules, which promote induction of defective structures, particularly coupled 5−8 ring defects, at the ice surface. Structural fluctuations promoted by these defective motifs assist hydrate cage formation next to the interface. The cage-like structures formed then act as a sink for methane molecules in the solution and enhance the stability and growth of an amorphous nucleus, which can evolve into a hydrate crystal upon annealing. These results are illustrative of how a surface that is structurally incompatible can serve to facilitate heterogeneous nucleation of a new crystalline phase. They should also further our general understanding of the formation of gas hydrates and their critical roles in various industrial and environmental processes, including carbon capture and storage.

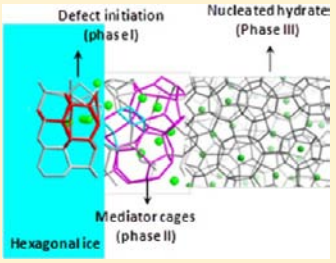

INTRODUCTION

Clathrate hydrates are a specific crystalline phase of aqueous solutions in which water molecules form cage-like structures, consisting primarily of five- and six-member rings around guest solutes.[1−5] Guest molecules, on the other hand, should conform a certain range of size to both fit into the water cages and stabilize them.[4,6,7] Low temperature, high pressure, and/or solute concentration are additional factors in the stabilization of clathrate hydrates.[2,4] Clathrate hydrates are found to form three primary types of crystalline structure known as structures I, II, and H.[4,6] The characteristic cages of these clathrate crystals include 5^{12}, $5^{12}6^2$, and $5^{12}6^4$, where the first cage is a common element among all hydrate crystals while the second and third are specific to structures I and II, respectively. Gas hydrates have received a great deal of attention because their structures provide promising options in energy storage and CO_2 sequestering.[4,5] Despite the potential applications and ubiquity of gas hydrates in nature, i.e., under permafrost in the Arctic and within ocean sediments,[1−5] many aspects of the molecular mechanisms associated with their homogeneous and heterogeneous nucleation and their growth are not yet well-understood. In the present work, we focus principally on the nucleation process of gas hydrates. The term "heterogeneous" will be used to refer to systems in which a solid interface with a fixed structure is introduced so that the behavior of a solution next to this solid surface is influenced.

Experimental studies of homogeneous nucleation of clathrate hydrates have proven to be very difficult due to the stochastic nature of the event and the lack of molecular-level time and spatial resolution.[6] In this regard, molecular simulations (molecular dynamics in particular) have been very successful in shedding lights on molecular details of nucleation, growth, dissociation, and structural stability of clathrate hydrates,[6] where possible roles of water rings/cages are of particular interest. Guo et al.[7−9] investigated the stability of 5^{12} cages and found that the concentration of methane molecules and the degree of supercooling can enhance the formation probability of 5^{12} cages. In addition, the same authors showed that there is a net attraction force for a solute being in a cage (i.e., a free energy difference between an encapsulated and a dissolved solute).[8] In parallel, the collective behavior of methane molecules observed in other molecular dynamics simulations suggests potential models to describe the mechanism of hydrate nucleation.[4,10−13] These simulations consistently indicate that methane and water molecules tend to organize upon an increase in the local density of methane. An organized aggregate of guest molecules in which solutes are separated by water molecules has been named a "blob".[10−13] As the density of methane molecules reaches a critical value, the probability of water cage formation (particularly a 5^{12} cage) is enhanced.[8,10−13] As fluctuations continue, an amorphous nucleus can form that can anneal into crystalline solids if they reach a critical size. This model has been termed the "blob mechanism".[10−13] Longer simulations (in the order of micro-seconds) with various system setups provided further support for the validity and generality of a two stage mechanism for the nucleation of gas hydrates.[14−20] Furthermore, through cage analyses, cage structures such as $5^{12}6^3$, $4^15^{10}6^2$, $4^15^{10}6^3$, and

Received: January 16, 2013
Published: April 22, 2013

   dx.doi.org/10.1021/ja400521e | J. Am. Chem. Soc. 2013, 135, 7278−7287

$4^1 5^{10} 6^4$, which are not found in a well-annealed hydrate crystal, have been identified during the process of nucleation.[15,16]

Heterogeneous nucleation of clathrate hydrates, on the other hand, has been well investigated experimentally. It is well established that the surface of hexagonal ice can facilitate hydrate nucleation in a heterogeneous process.[1] This phenomenon has been shown in experiments with ice powder/films,[1,21−26] differential scanning calorimetry (DSC) of hydrate-forming solutions,[27,28] and Raman microscopy.[29] When the surfaces of ice particles are exposed to a clathrate-forming gas, it is believed that the nucleation mechanism consists of two steps: (1) initial formation of a clathrate coating at the ice−gas interface and (2) subsequent growth of hydrate perpendicular to the interface as the core of the ice particle transforms into hydrate (shrinking core model).[26] Based on these experiments, hydrate formation on the surface of ice has been attributed to the reorganization of water molecules at the ice−gas interface[1,26] and explicitly on the existence of a quasi-liquid layer at the ice surface.[29] In the case of DSC experiments, depending on solution composition, the heat flux profiles indicate formation of an ice phase first, followed almost immediately by formation of a hydrate phase.[27,28] However, the resolution of these experiments were not high enough to provide any structural details of hydrate formation from solution in the presence of ice, and no models have been suggested for such a hydrate nucleation process. Therefore, to elucidate the molecular mechanism of hydrate nucleation next to the surface of ice further investigations are needed.

Computer simulations have been helpful in providing molecular-level insights into the structure of crystalline gas hydrates and hydrate nucleation next to solid surfaces. In this regard, investigation of the (001) face of a methane clathrate crystal[30] as well as nucleation of methane and carbon dioxide hydrates next to silica surfaces are worth mentioning.[31,32] Examination of the (001) face of a methane hydrate crystal revealed presence of various water rings (three- up to six-member rings) on the surface of the crystal that can result in formation of half-cages which may be closed by the clustering of more mobile water molecules.[30] Nucleation studies of hydrates next to silica surfaces have revealed a phenomenology with some characteristics similar to those observed for homogeneous nucleation, where a local increase in solute density next to the solid surface appears key in facilitating nucleation of an amorphous clathrate.[31,32] Even the cages observed during the nucleation process (prior to complete annealing) are similar to those reported for homogeneous nucleation.[31,32]

To date, there have been no investigations into the molecular-level mechanisms involved in the role of an ice surface in enhancing hydrate nucleation. In case of gas deposition on ice powders, there has been speculation[26,33] around possible roles of defects and vacancies, but the structural nature of such defects are yet to be clarified. Similar roles for surface defects seem probable in case of nucleation from solution next to ice. Recently, it has been demonstrated that the hexagonal ice−water interface is capable of exhibiting a particular type of defect, composed of coupled 5−8 rings,[34] where this defect appears to play an important role in stacking fault formation in ice in contrast to defects such as coupled 5−7 rings.[35]

In the present work, the heterogeneous nucleation of methane clathrate hydrate is investigated in the vicinity of the basal (0001) and prism (10−10) faces of hexagonal ice. Utilizing molecular dynamics simulations, we show that the surface of ice can promote nucleation of a clathrate hydrate. We monitor the population of rings and explore the configurations of system along the simulated trajectories at two different supersaturations of methane molecules and demonstrate that defect structures at the ice−solution interface play a key role in the nucleation process. The presented results offer a mechanistic understanding of clathrate hydrate formation in the presence of ice.[27,28,36] In addition, the present results illustrate the potential importance of defect structures in mediating connection/nucleation of otherwise structurally incompatible crystals.

SIMULATION DETAILS

Initial simulations were started with two-phase ice and water systems, where each phase occupied roughly half of the simulation box. The simulations boxes had dimensions of roughly 25 Å × 25 Å × 100 Å. Each system had two interfaces (due to periodic boundary conditions) perpendicular to the direction of heterogeneity, here labeled as the z-axis. In order to limit the formation of clathrate structures to one interface, a scheme developed for steady-state crystal growth simulation was employed (see Figure 1).[37] In this scheme, a

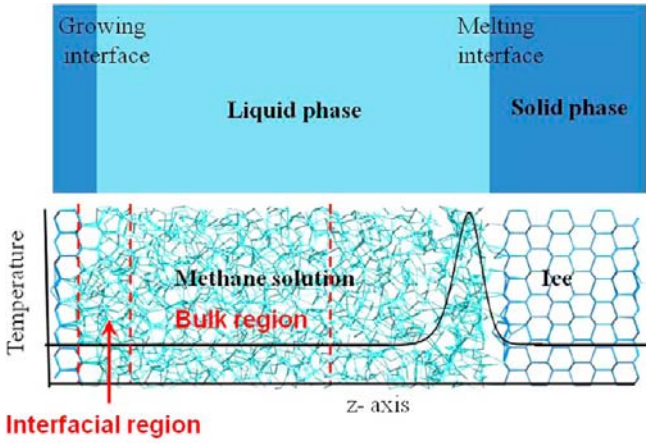

Figure 1. Schematic representation of the simulation setup. The top panel shows a schematic representation of the two-phase system with solid (dark blue) and liquid (cyan) regions along with two interfaces. The bottom panel presents a sample configuration of the system superimposed with the temperature profile across the system. The regions of interest, the ice−solution interface and bulk solution, are highlighted with red dashed lines. Further details are provided in the text.

temperature pulse (with a temperature maximum above the melting point of ice) was positioned next to one of the interfaces, while the rest of the system, including the other interface, was kept at constant undercooling. The six-site model of water was used in the present work since it has been shown that it reasonably captures the structural features of clathrate hydrate and ice crystals.[19,38] The united atom OPLS model was chosen for the methane molecules.[19,39] The cross interactions were estimated as geometric means.[39] The electrostatic interactions were evaluated using smooth particle mesh Ewald sums,[40] and a cutoff of 7.5 Å was considered for the van der Waals interactions.

Simulations were carried out at two concentrations of methane molecules. In one case, 50 water molecules in the liquid part of the system (with roughly 1000 water molecules) were randomly substituted with methane molecules, generating a solution of roughly 5 mol%. Six simulations were performed at this concentration, three of them with the basal face (0001) and three with the prism face (10−10) of hexagonal ice. For each face, the starting configuration was the same but the velocities were randomly assigned for each simulation.

dx.doi.org/10.1021/ja400521e | J. Am. Chem. Soc. 2013, 135, 7278−7287

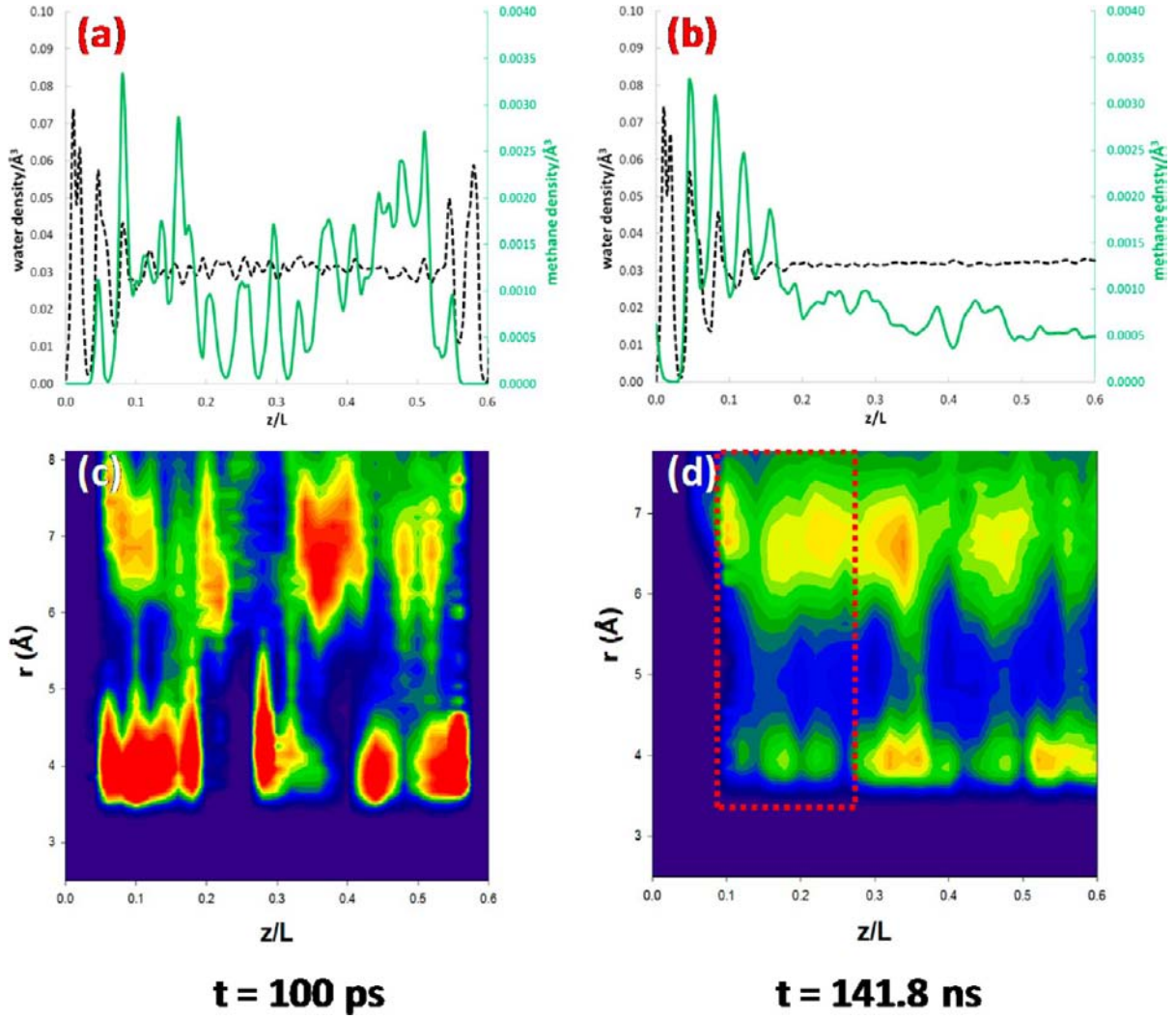

Figure 2. Time evolution of a methane solution next to the basal face of hexagonal ice. (a,b) Density profiles of methane and water molecules in a 5 mol% methane solution at 265 K next to the basal face of hexagonal ice near the beginning (100 ps) and at the end (141.8 ns) of the trajectory, respectively. The densities of water and methane molecules are represented with dashed black and solid green lines, respectively, along the direction of heterogeneity, z/L. (c,d) Radial distribution functions, $g_{C-C}(r)$, of methane molecules at 100 ps and 141.8 ns, respectively, as functions of the position of the central molecule in the simulation box, z/L, and the separation between methane molecules, r, where red corresponds to the highest values and blue to the lowest. The dotted rectangle in (d) highlights the interfacial region where the hydrate-like structures are evolving.

These systems were equilibrated for 5 ns and then simulations were run for at least 60 ns. Three of these trajectories, those exhibiting promising behavior, were run longer resulting in two runs of approximately 142 and 91 ns for the basal face and one of 163 ns for the prism face. In a second set of simulations, 100 methane molecules were randomly substituted for water molecules in the liquid region giving rise to an approximate concentration of 10 mol%. Two simulations were run at this concentration, one next to the basal face (45 ns) and one next to the prism face of hexagonal ice (35 ns). Both 5 and 10 mol% systems represent highly supersaturated conditions for the methane solution, and to avoid demixing of methane and water, the (mechanical) pressures were maintained at 500 and 1000 bar in the case of the 5 and 10 mol% systems, respectively, using a Berendson barostat.[41] The temperature across the system was set to 265 K, using Nosé–Hoover chain thermostats,[37,42] to ensure sufficient undercooling (estimated as roughly 40 K) relative to the melting temperature of the model methane hydrate to trigger the nucleation process on a molecular dynamics simulation time scale.[17,18]

To help identify phase transitions in the system, several parameters were monitored in addition to the potential energy of water molecules and the number density of both water and methane. A tetrahedral order parameter as well as the populations of water rings were investigated as suggested in earlier studies.[18,43] The tetrahedral order parameter employed,

$$S_g = \frac{3}{32}\sum_{j=1}^{3}\sum_{k=j+1}^{4}\left(\cos\psi_{j,k} + \frac{1}{3}\right)^2 \quad (1)$$

where $\psi_{j,k}$ is the angle between the oxygens of a central water molecule and its j and k closest neighbors, was introduced in ref 43. The procedure of identifying rings has been described elsewhere;[18,30,44] in brief, two water molecules were considered as hydrogen-bonded if they satisfied the criteria: (1) an O···H distance between 0.5 and 2.2 Å, (2) an OOH angle of less than 30°, and (3) an OOG angle greater than 110°, where G is the midpoint of the two water hydrogens on the bisector of the HOH angle.[44] An n-membered ring was then defined as an ordered sequence of n distinct water molecules connected to each other through H-bonds. Populations of five-member rings were used to detect formation of hydrate cages in a system.

Another parameter employed to help identify hydrate like structure in our systems was the radial distribution function for methane molecules.[13,45] According to ref 13, the radial distribution function between methane carbons, $g_{C-C}(r)$, has peaks around 4 and 7 Å for a methane solution corresponding to direct contact and solvent-

dx.doi.org/10.1021/ja400521e | J. Am. Chem. Soc. 2013, 135, 7278–7287

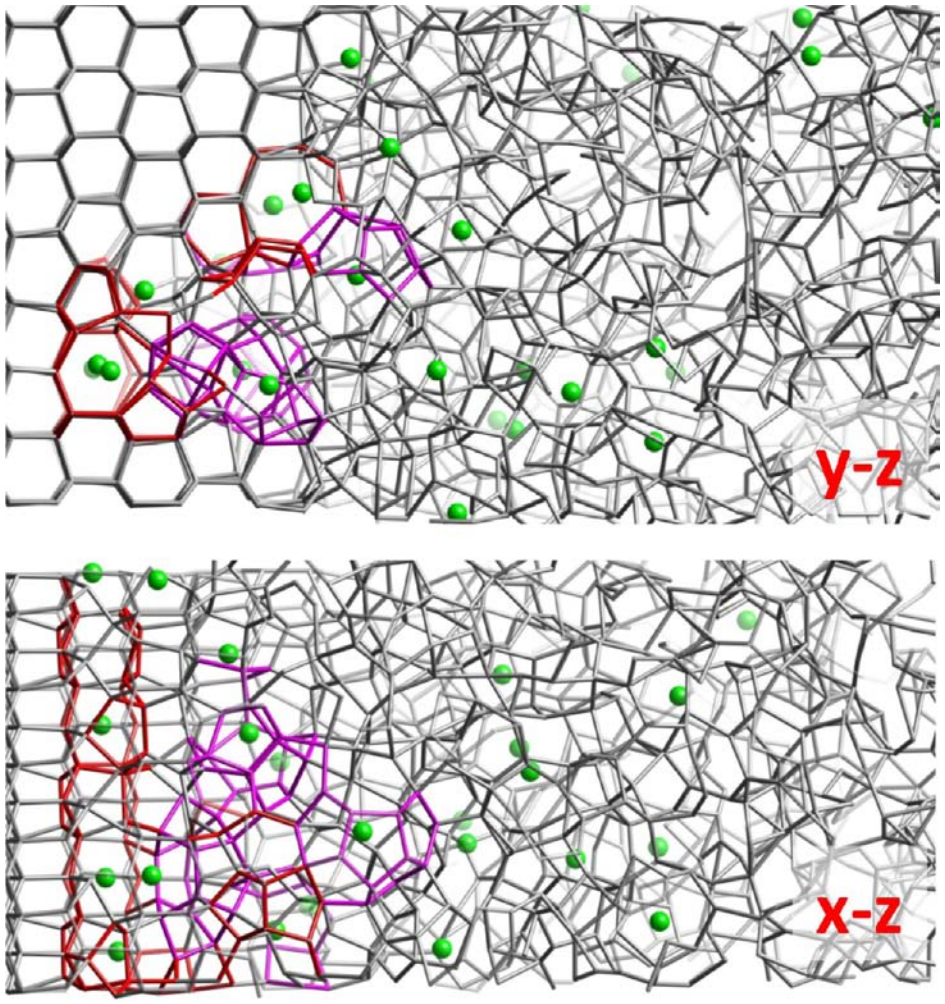

Figure 3. Behavior of a methane solution next to the basal face of hexagonal ice at 265 K. This configuration (averaged over a 100 ps time window) was recorded at 90.5 ns of an independent trajectory. The two different orientations highlight the development of coupled 5−8 ring defects and of clathrate half-cages, shown with red and magenta sticks, respectively. The intrusion of liquid into the ice is notable. The corresponding density profiles and methane radial distribution function of this configuration are provided in SI-Figure 1.

separated methane molecules, respectively. Upon formation of clathrate hydrate structure in the system, the peak at 4 Å disappears and the peak around 7 Å grows and its maximum shifts toward a separation of about 6 Å.[13,45] In the present work, to help track the nucleation process of clathrate structure, the aqueous part of the system was divided into two main regions, interface and bulk (schematically presented in Figure 1). The radial distribution function of methane molecules was averaged over each of these regions. The $g_{C-C}(r)$ was also binned along the direction of heterogeneity (according to the z position of the central methane) to further clarify the ordering of methane molecules in different locations in the system. Sample configurations were chosen along trajectories and were carefully inspected for cage structure for the purpose of visualization.

RESULTS AND DISCUSSION

Figure 2 presents the average density and radial distribution function of methane molecules at the start and end of one of the simulation trajectories of a 5 mol% methane system next to the basal face of ice. At 0.1 ns (Figure 2a), methane molecules were reasonably randomly distributed along the direction of heterogeneity, identified as z/L, where L is the length of the simulation box along the z-axis and is about 100 Å for the present systems. After roughly 142 ns of simulation, it can be observed that methane molecules have accumulated near the ice−water interface (Figure 2b). An enhancement of methane density at the ice−water interface relative to the bulk solution is apparently thermodynamically favored; this is consistent with corresponding decreases in the free energy of a methane molecule going from gas phase to either the water or ice interface, verified both experimentally[46] and through simulations.[47,48] The migration of methane molecules toward ice is accompanied by their organization within the ice−water interfacial region. It can be seen from the density profile in Figure 2b that methane molecules tend to appear in layers in the vicinity of the basal face. Additionally, examination of the radial distribution function of methane molecules, $g_{C-C}(r)$, reveals that methane molecules had the expected solution-like arrangements at the beginning of the simulation (dominance of the contact peak around 4 Å in Figure 2c).[45] As time elapses and the local density of methane molecules increases next to the ice−water interface, the local arrangement of methane molecules begins to change. The reduction of the contact peak in the radial distribution function around 4 Å and the enhancement of the solvent-separated solute peak at r = 6−7 Å suggests development of a more clathrate hydrate-like structure next to the ice surface (see Figure 2d).[27]

dx.doi.org/10.1021/ja400521e | J. Am. Chem. Soc. 2013, 135, 7278−7287

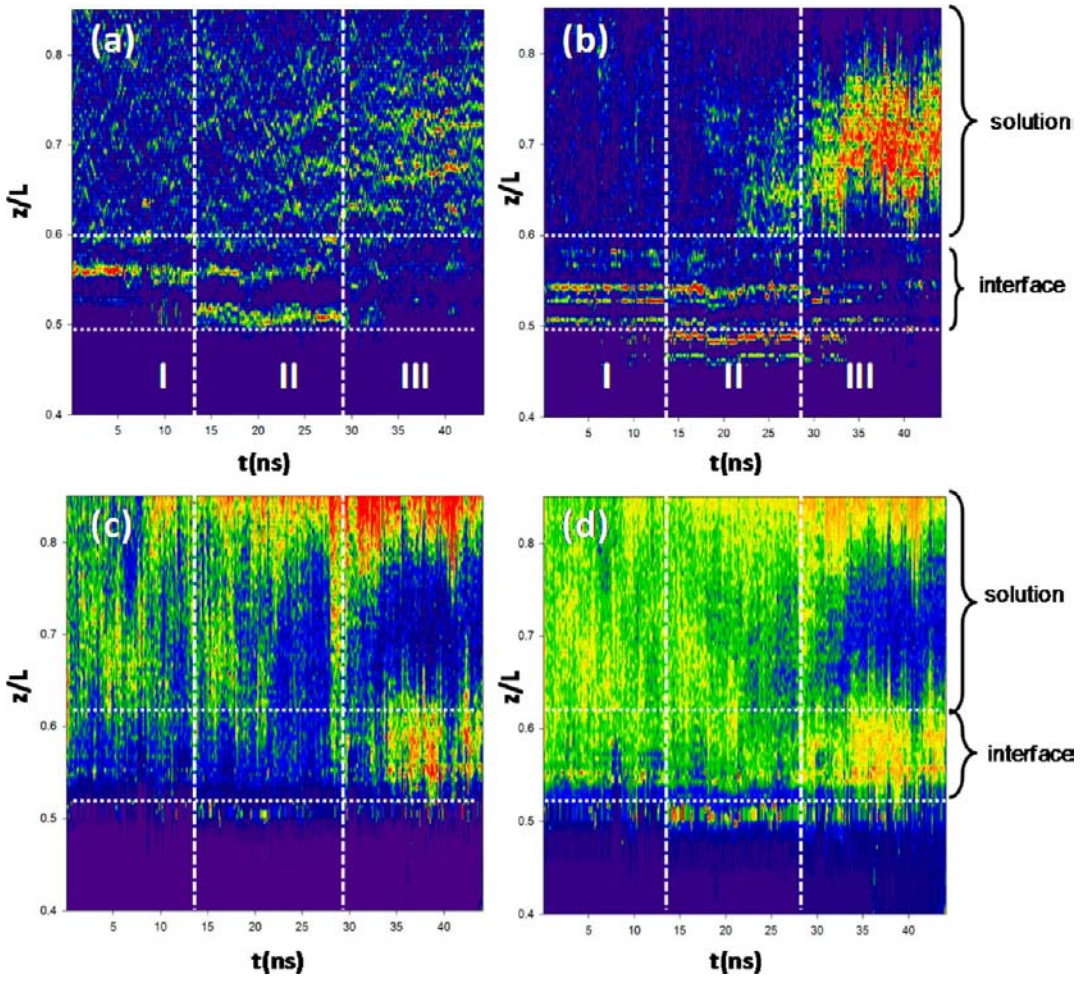

Figure 4. Temporal evolution of various properties of a solution with 10 mol% methane during hydrate nucleation next to the basal face of hexagonal ice at 265 K. Time dependence of four different measures resolved along the direction of heterogeneity, where the horizontal and vertical axes are the time and the position, z/L, in the simulation box, respectively. (a) Density of methane molecules and (b) population of five-member rings, respectively, in which red corresponds to the highest population or density and blue to the lowest. (c) Tetrahedral order parameter, S_g, and (d) potential energy of water molecules, respectively, where red color corresponds to liquid-state values and blue to solid-state (ice and hydrate) values. The white dotted lines represent the boundaries of the interface and solution regions. The trajectory is divided into three stages (denoted as I, II, and III in panels (a) and (b) and delimited by white dashed lines), which will be defined in Figure 8. In this analysis, all configurations were aligned so that the last layer of the ice crystal is at z/L = 0.5.

Looking at the configurations of such systems reveals that there are hydrate-like motifs next to the ice surface, which are coupled to defects formed in the presence of methane molecules. Figure 3 presents snapshots from another 5 mol% system next to the basal face. In this system, after roughly 90.5 ns, methane molecules have also accumulated next to the ice–water interface. The radial distribution function of methane molecules (for this system see SI-Figure 1b) within the interfacial region again shows enhancement of hydrate-like features. In this second system, methane molecules have induced a massive defect structure on the ice surface (see Figure 3). A major component of these irregularities in the ice surface is the coupled 5–8 ring defect.[34] It can be seen that there are cage-like structures, evident primarily as half-cages in Figure 3, attached to the coupled 5–8 ring defects. These results indicate that coupled 5–8 ring defects can play an important role in promoting hydrate-like structures next to the ice surface.

In a very recent study Knott et al.[49] have demonstrated that homogeneous nucleation rates of methane hydrate are extremely low unless highly elevated supersaturations are utilized. Previous investigations[19] of homogeneous nucleation of methane hydrates have shown that the nucleation of methane hydrate can proceed rapidly upon reaching a critical local methane density of 0.003 Å^{-3}. The locally high concentration of methane promotes the restructuring of the water molecules surrounding the methane molecules, and elements of clathrate cages become apparent.[10−19] Density profiles for the present 5 mol% systems (see Figure 2a and SI-Figure 1a) indicate that even in regions of high local concentration, the methane density only approaches the lower bound for the critical concentration apparently needed for (rapid) nucleation of a methane clathrate hydrate. Therefore, on the time scale of our simulations, only the development of short-range clathrate-like structures might be expected to be observed. This is further supported by the fact that only three of the six 5 mol% systems appeared to develop hydrate-like motifs. To help drive the nucleation process, systems with twice the solution concentration (i.e., 10 mol%) were examined. It should be emphasized that even with 100 methane molecules the concentration of the solution phase is

dx.doi.org/10.1021/ja400521e | J. Am. Chem. Soc. 2013, 135, 7278−7287

still less than those in previous simulations exploring homogeneous nucleation of methane hydrate.[15−17]

Figure 4 presents the results of the simulation of a 10 mol% methane solution next to the basal face of hexagonal ice. Four important properties of the system were monitored as functions of time and across the direction of heterogeneity: the local density of methane molecules (Figure 4a), the population of five-member rings (Figure 4b), the tetrahedrality of the four nearest neighbors of water molecules (Figure 4c), and the potential energy of water molecules (Figure 4d). Although initially methane molecules were randomly scattered in the solution, they relatively quickly migrate toward the ice−water interface (similar to the 5 mol% systems); consequently, the local concentration of methane molecules increases within the interfacial region and begins to affect the structure of water molecules in this region. The increased methane density enhances the population of five-member rings (major structural component of hydrate cages) within the interfacial region, as is evident from Figure 4b. In this simulation, the accumulation of methane and the subsequent increase in the population of five-member rings take place between 15 and 30 ns. Beyond 25 ns, it seems that the methane molecules begin to leave the interfacial region (their density starts to decrease) in favor of the solution region. At the same time, the population of five-member rings in the solution region begins to increase. Inspecting Figure 4c,d also reveals that between 25 and 30 ns, the water molecules in the solution region become more tetrahedrally ordered and their potential energy decreases. It seems reasonable to argue that the period of 25−30 ns corresponds to a key point in the evolution of this system. During this period, structural fluctuations start to arrange the water molecules into cage-like structures that help support the locally increased concentration of methane. After 30 ns, methane molecules appear to form more organized layers (see Figure 4a). This layering is accompanied by a dramatic increase in the population of five-member rings (see Figure 4b), which is indicative of nucleation of a new phase, specifically an amorphous methane clathrate hydrate.[10−19] As can be seen in Figure 4c,d, the water molecules in the new amorphous hydrate phase are more tetrahedrally ordered relative to the liquid phase, and their energetic stability is comparable to that in the ice phase. However, it is important to note that despite the transient structural connections between the ice and hydrate between 25 and 30 ns, the hydrate phase eventually separates itself from the ice, leaving a disordered liquid-like region of water molecules between the two solid phases. The structural mismatch between ice and hydrate accounts for this liquid-like region. Similar trends have been observed for the same local properties in the case of the 10 mol% system next to the prism face of hexagonal ice (see SI-Figure 2).

To investigate further the formation of the new hydrate phase, the evolution of the radial distribution function of methane molecules (as averaged over a particular region) has also been monitored both within the interfacial region and in the bulk solution. Figure 5 shows that methane molecules have a solution-like arrangement (i.e., there are significant numbers of contact pairs) at the beginning of the simulation (similar to Figure 2c), both in the interface and solution regions.[45] As time evolves, the interfacial region exhibits a transition in which organization of the methane molecules becomes more hydrate-like (i.e., where solvent-separated methane molecules dominate), corresponding to the accumulation of methane molecules within the interfacial region seen in Figure 4a. The

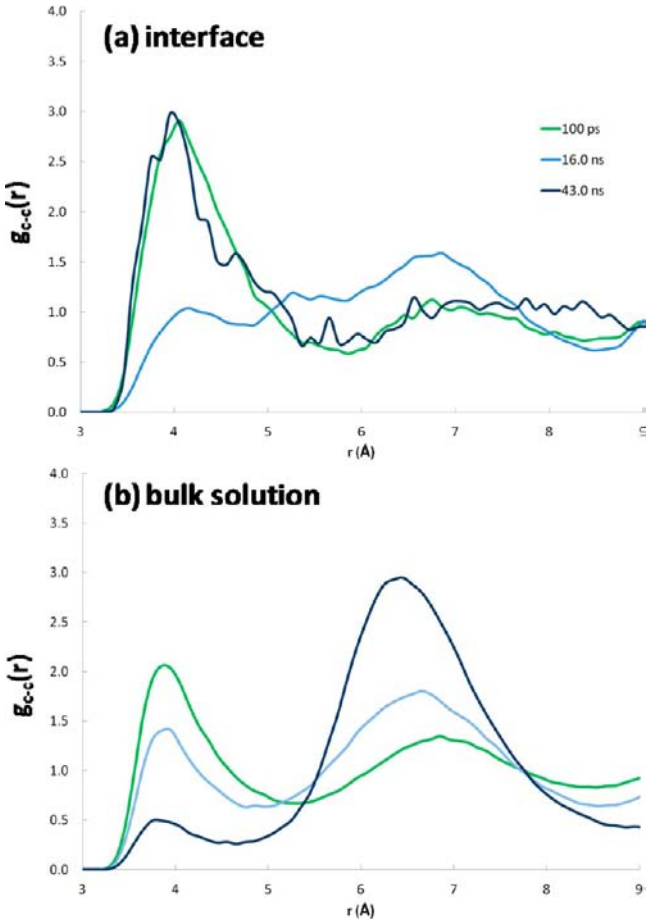

Figure 5. Evolution of the radial distribution function of a 10 mol% methane solution next to the basal face of hexagonal ice at 265 K. The radial distribution functions, $g_{C-C}(r)$, of methane molecules are shown in two regions of interest, (a) interface and (b) bulk solution, as denoted in Figure 4. The 100 ps (green) and 43.0 ns (dark blue) lines correspond to the beginning and the end of the simulation trajectory, respectively.

solvent-separated peak in $g_{C-C}(r)$ for the solution region only becomes dominant later in the simulation trajectory. Once hydrate-like features have been established in the bulk solution region, however, the $g_{C-C}(r)$ for methane molecules in the interfacial region returns to apparent solution-like behavior, with the contact peak again being dominant. The evolution of the radial distribution function for the 10 mol% system next to the prism face shows a similar trend and can be found in SI-Figure 3.

To provide further microscopic insights, configurations of the nucleating phase next to the prism face at different stages of its evolution are presented in Figure 6. It can be noted from this figure that as time elapses various types of cages have appeared. The highlighted cages, including 5^{12}, $5^{12}6^2$, $5^{11}6^24^1$, $5^{12}6^4$, and $5^{12}6^3$ (also see SI-Figure 4), are indicative of formation of an amorphous solid phase as similar cage structures have previously been observed during homogeneous nucleation of methane hydrates.[10−19] Empty cages, which have been observed in earlier simulations,[13] were also noted in the structure of the nucleating hydrate phase next to the prism face of ice (see SI-Figure 4 for a cross-sectional view of the configuration at 35.0 ns).

dx.doi.org/10.1021/ja400521e | J. Am. Chem. Soc. 2013, 135, 7278−7287

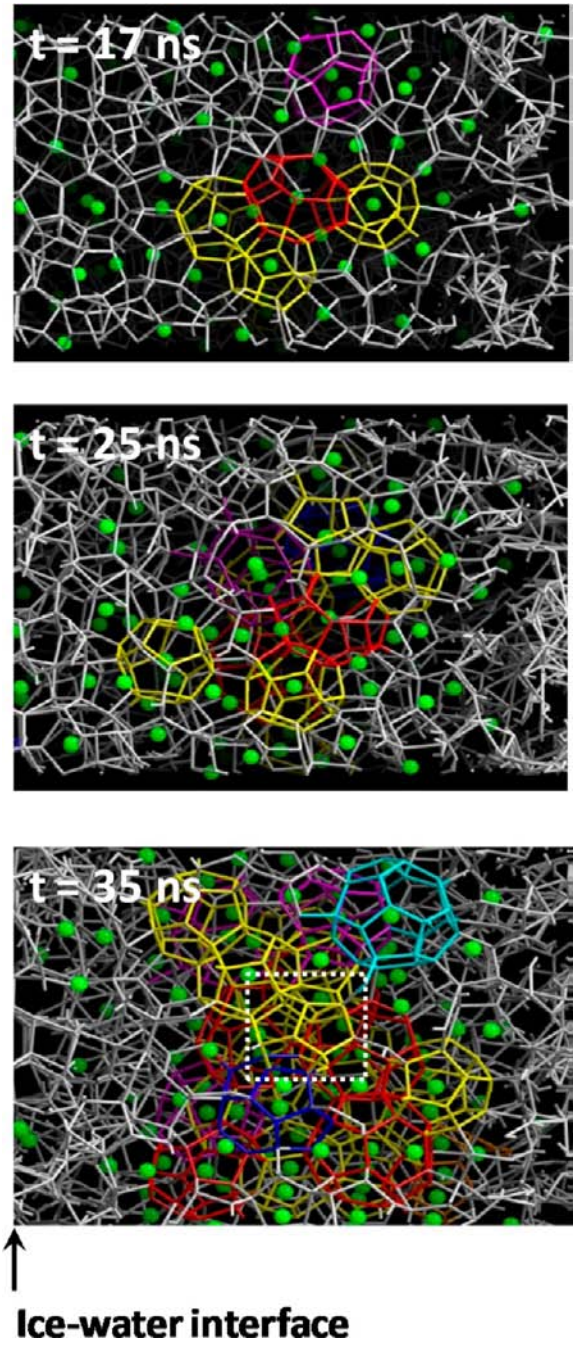

Figure 6. Configurations from a simulation trajectory of a 10 mol% methane solution next to the prism face of hexagonal ice. Averaged configurations of the solution region of the system, sliced along the *y*–*z* plane, are presented, where the corresponding time indices are provided. In these snapshots, 5^{12}, $5^{12}6^2$, and $5^{12}6^4$ cages have been colored yellow, red, and cyan, respectively. The white dotted square highlights an empty 5^{12} cage. Half-cages and cages with seven-member rings or larger are presented with magenta and orange sticks, respectively. An *x*–*y* plane cross-sectional view of the configuration at 35.0 ns is provided in SI-Figure 4.

As mentioned earlier, methane hydrate structure has flat five-member water rings as a major structural element. Therefore, a structural transitioning element would be necessary for ice (consisting of puckered six-member rings) to serve as a platform for hydrate nucleation. Inspecting the simulation trajectories for both 5 and 10 mol% methane solutions indicates that the accumulation of methane molecules enhances the probability of coupled 5–8 ring defect formation.[34] This defect features a pair of coupled five-member rings which can serve as a pattern for further formation of five-member rings.[34] Additionally, the eight-member ring voids can serve as relatively stable locations for methane molecules to occupy (similar to hydrate half-cages). The accumulation of methane molecules in these defects will help to order the neighboring water molecules. Figure 7 presents configurations of different 10

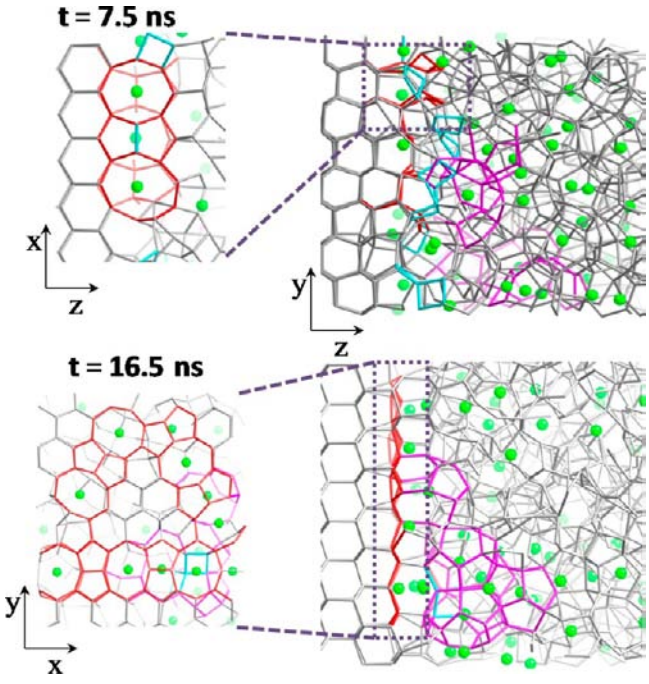

Figure 7. Structure at the ice surface prior to nucleation of hydrate. Sample configurations of the ice–solution interface next to the prism face at 7.5 ns (top) and the basal face at 16.5 ns (bottom) are presented. Configurations of the former system are those shown in Figure 5. The gray sticks represent hydrogen bonds between water molecules. The coupled 5–8 ring defects, four-member rings, and distorted/irregular/half-cages are colored red, cyan, and magenta, respectively. Methane molecules are presented as green spheres. The insets in the top and bottom panels show *x*–*z* and *x*–*y* cross sections of coupled 5–8 ring defects, respectively.

mol% methane solution systems (in addition to Figure 3), where coupled 5–8 ring defects are shown together with their connection to the neighboring hydrate-like cages. It is also observed that the presence of a methane in an 8-member ring void can lead to water molecules completing the cap of the void, similar to what was observed by Chihaia et al.[30] in case of the (001) face of methane hydrate (see the top panel of Figure 7). This observation indicates that the coupled 5–8 ring defect can be a local arrangement on the ice surface that helps mediate the structural conversion from ice to hydrate. It should be noted that an increased population of four-member rings (at least twice that of a pure ice–water system) was also found. This elevated occurrence of four-member rings is consistent with other simulations in which the homogeneous nucleation of hydrate was investigated.[28–30]

Upon consideration of our findings for the 5 mol% systems in combination with the results in Figure 4 (and SI-Figure 2), we propose a three-stage mechanism for the heterogeneous nucleation of a gas hydrate in the presence of hexagonal ice.

dx.doi.org/10.1021/ja400521e | J. Am. Chem. Soc. 2013, 135, 7278–7287

Figure 8 schematically summarizes this mechanism which we denote as IPN (induce–promote–nucleate). In the first step of

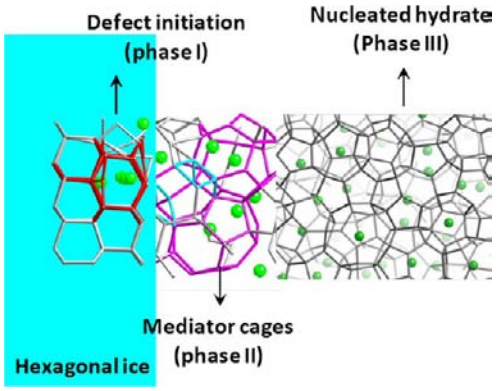

Figure 8. "IPN" mechanism of heterogeneous hydrate nucleation. The role of ice in the heterogeneous nucleation of methane clathrate hydrate can be described by a three stage mechanism. In phase I, a defect structure is induced (the coupled 5–8 ring defect) on the surface of ice, promotion of cage-like structures from the defective regions into the bulk solution occurs during phase II, and in phase III methane and water molecules organize during the formation of an initial (amorphous) hydrate nucleus.

the IPN mechanism, methane molecules accumulate within the interfacial region of the ice. Their relatively high concentration distorts the structure of the ice surface and induces coupled 5–8 ring defects (see phase I of Figure 8). Formation of such defects with associated methane molecules helps to order water molecules, and cage-like structural fluctuations are promoted in the vicinity of the interfacial region (see phase II of Figure 8). These structural fluctuations propagate into the solution region and couple to elevated levels of local methane concentration. Hydrate-like cages become numerous and persistent (in time), and eventually an amorphous hydrate-like solid forms where the local methane concentration approaches that of a crystalline hydrate. It is important to note that other studies have shown that such amorphous hydrate-like solids will anneal to more recognizable crystalline hydrate forms under appropriate conditions.[10,11,13−20] Once formed, the new hydrate phase acts as a sink for the rest of the methane molecules in the system, depleting the ice–water interfacial region of methane and separating itself from the ice (see phase III of Figure 8). These three stages are denoted in Figure 4 (and SI-Figure 2) with vertical white dashed lines.

The results of this study are consistent with recent work on nucleation of clathrate hydrates next to silica surfaces.[31,32,48] Silica, like ice, does not have a structural match with the hydrate yet can apparently provide support for clathrate hydrate nucleation. Accumulation of guest molecules and associated structural fluctuations next to a silica surface have been observed to lead to formation of clathrate-like cages in a process similar to that visualized here next to the ice–water interface.[32] These consistent observations demonstrate the need of mediator structures (such as $5^{12}6^3$ cages in the cross nucleation of sI and sII gas hydrates[50,51]) in a heterogeneous nucleation process where the substrate and the new solid phase are structurally not in register. In the case of ice, the coupled 5–8 ring defect appears to be able to play this role as its structural features can bridge those of ice and a clathrate hydrate.

The observations presented in this work are in qualitative agreement with various aspects of very recent studies of nucleation of clathrate hydrates.[29,46,48,49,52] The present results emphasize the crucial role played by the interfacial region at the ice surface. The apparently enhanced solubility of methane molecules at the ice–water interface increases the local composition of guest molecules, which when coupled with structural fluctuations helps to trigger hydrate formation, consistent with phenomenology seen in experiments.[29,46] We note that in the experimental work of Boewer et al.[46] an accumulation of guest molecules (Xe and CO_2) was found inside a nanometer thick interfacial layer at the water interface, where these particular systems exhibited more rapid hydrate nucleation. In a simulation study of the quasi-liquid layer (QLL) on the surface of ice using coarse-grain models, Shepherd et al.[53] did not note an enhancement of the solubility of methane relative to the bulk liquid at the same temperature. It is unclear if the apparent difference with the current results is due to differences in the models, or if the behavior of the QLL will only asymptotically approach bulk system behavior. As mentioned above, the current bulk concentrations are highly supersaturated, although not as highly as the systems in previous simulation studies.[15−17] Knott et al.[49] have shown that homogeneous nucleation is an extremely rare event under driving force conditions consistent with typical experiments. These authors have concluded that the experimental rates of hydrate nucleation (as well as those found in environments such as permafrost or pipelines) are likely determined by heterogeneous processes, and hence by the presence of surfaces.[49] The present results suggest that in the presence of surfaces, in this case that of ice, the nucleation of a gas hydrate can be considerably enhanced (relative to the homogeneous process at the same conditions). The possible influence of temperature on the mechanism of hydrate nucleation should also be discussed in view of very recent work. The results present here have been obtained from a set of simulations in which the temperature was strictly controlled. The thermostats employed in these simulated systems facilitate formation of clathrate-like structures by immediately removing the heats of formation of hydrate cages. Liang and Kusalik[52] have very recently observed that a hydrate forming system under NVE conditions, while exhibiting similar qualitative behavior, nucleates somewhat more slowly but gives rise to better quality (i.e., more crystalline) structures. They conjecture that the increasing temperature of the system, as nucleation proceeds, aids in annealing of the structure that forms. We might expect similar behavior to be observed if the current systems were simulated under NVE conditions, where the temperature would rise until it reaches the ice melting point, after which time hydrate would form at the expense of ice melting. As a last point, we might speculate that a particular exposed face of an ice crystal might bias the nucleation process toward a particular orientation of the resulting methane hydrate crystal. Since we anticipate this to be a subtle effect, it is likely to be extremely challenging to characterize.

■ CONCLUSIONS

We have investigated the molecular origins of clathrate hydrate nucleation from a solution phase next to the surface of hexagonal ice. We have explicitly examined the case of a methane solute guest, however the framework reported here can easily be generalized to other relevant guest molecules. Our results and observations can be summarized with a three-step

dx.doi.org/10.1021/ja400521e | J. Am. Chem. Soc. 2013, 135, 7278–7287

IPN (induce−promote−nucleate) mechanism for the heterogeneous nucleation process. The IPN mechanism proposes that methane molecules initially migrate toward the ice−solution interface, and then induce structural changes composed of coupled 5−8 ring defects[34] (induction phase). The structural elements of this defect provide temporary support for the promotion of fluctuations involving cage-like structures. These cage-like structures are reasonably long-lived due to their connection to surface defects of the ice and eventually facilitate nucleation of an amorphous hydrate-like solid. This solid can be expected to anneal to a more recognizable hydrate crystal on a time scale beyond that of the present simulations.[10−19] The observations made here are also consistent with the recent "blob mechanism" model[10−13] that suggests local fluctuations in density of guest molecules can give rise to formation of clusters and amorphous precursors.[19,54] By increasing the formation probability of hydrate-like structures (i.e., distorted, irregular or half-cages) in the vicinity of defective regions of ice, the surface of ice was observed to drastically shorten the expected nucleation time compared to homogeneous processes.[14−17]

The presented results can also provide more general insights into heterogeneous nucleation of solid phases on surfaces with nonmatching lattice structures. An obvious case is the experimental observation of ice particles facilitating hydrate nucleation from vapor or within solution (studied here). It seems that formation of specific defects (the coupled 5−8 ring defect) can facilitate such nucleation processes. We conjecture that similar defects exist on the surfaces of ice particles, and when exposed to hydrate-forming gases, they can serve as nucleating centers leading to formation of the clathrate hydrate coat. These results may also help to provide insights for scientists and engineers to design and fabricate appropriate surfaces to act as hydrate nucleators (e.g., for storage of carbon dioxide), or as inhibitors of clathrate hydrates by minimizing the probability of methane accumulation and molecular structures facilitating hydrate crystallization (e.g., for flow assurance in oil pipelines).

■ ASSOCIATED CONTENT

Supporting Information

Density profiles and $g_{C-C}(r)$ related to Figure 2; time evolution of methane density, five-member rings population, tetrahedral order parameter, potential energy of water molecules, and spatially averaged $g_{C-C}(r)$ of a 10 mol% solution next to the prism face of hexagonal ice; and $x-y$ cross-sectional view of Figure 5 at 35 ns. This material is available free of charge via the Internet at http://pubs.acs.org.

■ AUTHOR INFORMATION

Corresponding Author

pkusalik@ucalgary.ca

Notes

The authors declare no competing financial interest.

■ ACKNOWLEDGMENTS

The authors acknowledge support from the National Science and Engineering Research Counsel of Canada (NSERC), University of Calgary, and Westgrid computational facility.

■ REFERENCES

(1) Sloan, E. D., Jr.; Fleyel, F. *AIChE J.* **1991**, *37*, 1281−1292.
(2) Barrer, R. M.; Ruzicka, D. J. *Trans. Faraday Soc.* **1962**, *58*, 2262−2271.
(3) Holder, G. D.; Zele, S.; Enick, R.; LeBlond, C. *Ann. N.Y. Acad. Sci.* **1994**, *715*, 344−353.
(4) Hawtin, R. W.; Quigley, D.; Rodger, P. M. *Phys. Chem. Chem. Phys.* **2008**, *10*, 4853−4864.
(5) Anderson, B. J.; Radhakrishnan, R.; Peters, B.; Borghi, G. P.; Tester, J. W.; Trout, B. L. In *Physics and Chemistry of Ice*; Kuhs, W. F., Ed.; The Royal Society of Chemistry: Cambridge, 2007; pp 3−12.
(6) Sum, K. A.; Koh, C. A.; Sloan, E. D. *Ind. Eng. Chem. Res.* **2009**, *48*, 7457−7465.
(7) Guo, G. J.; Zhang, Y. G.; Li, M.; Wu, C. H. *J. Chem. Phys.* **2008**, *128*, 194504.
(8) Guo, G. J.; Li, M.; Zhang, Y. G.; Wu, C. H. *Phys. Chem. Chem. Phys.* **2009**, *11*, 10427−10437.
(9) Guo, G.-J.; Zhang, Y.-G.; Liu, H. *J. Phys. Chem. C* **2007**, *111*, 2595−2606.
(10) Jacobson, L. C.; Molinero, V. *J. Am. Chem. Soc.* **2011**, *133*, 6458−6463.
(11) Jacobson, L. C.; Hujo, W.; Molinero, V. *J. Am. Chem. Soc.* **2010**, *132*, 11806−11811.
(12) Jacobson, L. C.; Hujo, W.; Molinero, V. *J. Phys. Chem. B* **2009**, *113*, 10298−10307.
(13) Jacobson, L. C.; Hujo, W.; Molinero, V. *J. Phys. Chem. B* **2010**, *114*, 13796−13807.
(14) Walsh, M. R.; Koh, C. A.; Sloan, E. D.; Sum, A. K.; Wu, D. T. *Science* **2009**, *326*, 1095−1098.
(15) Walsh, M. R.; Rainey, J. D.; Lafond, P. G.; Park, D. H.; Beckham, G. T.; Jones, M. D.; Lee, K. H.; Koh, C. A.; Sloan, E. D.; Wu, D. T.; Sum, A. K. *Phys. Chem. Chem. Phys.* **2011**, *13*, 19951−19959.
(16) Guo, G. J.; Zhang, Y. G.; Liu, C. J.; Li, K. H. *Phys. Chem. Chem. Phys.* **2011**, *13*, 12048−12057.
(17) Walsh, M. R.; Beckham, G. T.; Koh, C. A.; Sloan, E. D.; Wu, D. T.; Sum, A. K. *J. Phys. Chem. C* **2011**, *115*, 21241−21248.
(18) Sarupria, S.; Debenedetti, P. G. *J. Phys. Chem. Lett.* **2012**, *3*, 2942−2947.
(19) Vatamanu, J.; Kusalik, P. G. *Phys. Chem. Chem. Phys.* **2010**, *12*, 15065−15072.
(20) Liang, S.; Kusalik, P. G. *Chem. Sci.* **2011**, *2*, 1286−1292.
(21) Pietrass, T.; Gaede, H. C.; Bifone, A.; Pines, A.; Ripmeester, J. A. *J. Am. Chem. Soc.* **1995**, *117*, 7520−7525.
(22) Moudrakovski, I. L.; Ratcliffe, C. I.; McLaurin, G. E.; Simard, B.; Ripmeester, J. A. *J. Phys. Chem. A* **1999**, *103*, 4969−4972.
(23) Chan, J.; Forrest, J. A.; Torrie, B. H. *J. Appl. Phys.* **2004**, *96*, 2980−2984.
(24) Kuhs, W. F.; Staykova, D. K.; Salamatin, A. N. *J. Phys. Chem. B* **2006**, *110*, 13283−13295.
(25) Staykova, D. K.; Kuhs, W. F.; Salamatin, A. N.; Hansen, T. *J. Phys. Chem. B* **2003**, *107*, 10299−10311.
(26) Falenty, A.; Genov, G.; Hansen, T. C.; Kuhs, W. F.; Salamatin, A,N. *J. Phys. Chem. C* **2011**, *115*, 4022−4032.
(27) Zhang, Y.; Debenedetti, P. G.; Prud'homme, R. K.; Pethica, B. A. *J. Phys. Chem. B* **2004**, *108*, 16717−16722.
(28) Davies, S. R.; Hester, K. C.; Lachance, J. W.; Koh, C. A.; Sloan, E. D. *Chem. Eng. Sci.* **2009**, *64*, 370−375.
(29) Muro, M.; Harada, M.; Hasegawa, T.; Okada, T. *J. Phys. Chem. C* **2012**, *116*, 13296−13301.
(30) Chihaia, V.; Adams, S.; Kuhs, W. F. *Chem. Phys.* **2005**, *317*, 208−225.
(31) Bai, D.; Chen, G.; Zhang, X.; Wang, W. *Langmuir* **2011**, *27*, 5961−5967.
(32) Liang, S.; Rozmanov, D.; Kusalik, P. G. *Phys. Chem. Chem. Phys.* **2011**, *13*, 19856−19864.
(33) Yinnon, C. A.; Buch, V.; Devlin, J. P. *J. Chem. Phys.* **2004**, *120*, 11200−11208.
(34) Pirzadeh, P.; Kusalik, P. G. *J. Am. Chem. Soc.* **2011**, *133*, 704−707.
(35) Grishina, N.; Buch, V. *J. Chem. Phys.* **2004**, *120*, 5217−5225.

(36) Davies, S. R.; Lachance, J. W.; Sloan, E. D.; Koh, C. A. *Ind. Eng. Chem. Res.* **2010**, *49*, 12319−12326.
(37) Vatamanu, J.; Kusalik, P. G. *J. Chem. Phys.* **2007**, *126*, 124703.
(38) Nada, H.; van der Eerden, J. P. J. M. *J. Chem. Phys.* **2003**, *118*, 7404−7413.
(39) Jorgensen, W. L.; Madura, J. D.; Swenson, C. J. *J. Am. Chem. Soc.* **1984**, *106*, 6638−6646.
(40) Essmann, U.; Perera, L.; Berkowitz, M. L.; Darden, T.; Lee, H.; Pedersen, L. G. *J. Chem. Phys.* **1995**, *103*, 8577−8593.
(41) Berendsen, H. J. C.; Postma, J. P. M.; Vangunsteren, W. F.; Dinola, A.; Haak, J. R. *J. Chem. Phys.* **1984**, *81*, 3684−3690.
(42) Martyna, G. J.; Klein, M. L.; Tuckerman, M. *J. Chem. Phys.* **1992**, *97*, 2635−2643.
(43) Chau, P. L.; Hardwick, A. J. *Mol. Phys.* **1998**, *93*, 511−518.
(44) Pirzadeh, P.; Beaudoin, E. N.; Kusalik, P. G. *Chem. Phys. Lett.* **2011**, *517*, 117−125.
(45) Yasuoka, K.; Murakoshi, S. *Ann. N.Y. Acad. Sci.* **2000**, *912*, 678−684.
(46) Boewer, L.; Nase, J.; Paulus, M.; Lehmkühler, F.; Tiemeyer, S.; Holz, S.; Pontoni, D.; Tolan, M. *J. Phys. Chem. C* **2012**, *116*, 8548−8553.
(47) Partay, L. B.; Jedlovszky, P.; Hoang, P. N. M.; Picaud, S.; Mezei, M. *J. Phys. Chem C* **2007**, *111*, 9407−9416.
(48) Bagherzadeh, S. A.; Englezos, P.; Alavi, S.; Ripmeester, J. A. *J. Phys. Chem. C* **2012**, *116*, 24907−24915.
(49) Knott, B. C.; Molinero, V.; Doherty, M. F.; Peters, B. *J. Am. Chem. Soc.* **2012**, *134*, 19544−19547.
(50) Vatamanu, J.; Kusalik, P. G. *J. Am. Chem. Soc.* **2006**, *128*, 15588−15589.
(51) Nguyen, A. H.; Jacobson, L. C.; Molinero, V. *J. Phys. Chem. C* **2012**, *116*, 19828−19838.
(52) Liang, S.; Kusalik, P. G. *J. Phys. Chem. B* **2013**, *117*, 1403−1410.
(53) Shepherd, T. D.; Koc, M. A.; Molinero, V. *J. Phys. Chem. C* **2012**, *116*, 12172−12180.
(54) Unwin, P. R. *Faraday Discuss.* **2007**, *136*, 409−416.